Nanomanufacturing of Tobacco Mosaic Virus-Based Spherical Biomaterials Using a Continuous Flow Method

Michael A. Bruckman,[†] Allen VanMeter,[†] and Nicole F. Steinmetz*[†,‡,§,⊥]

[†]Department of Biomedical Engineering, [‡]Department of Radiology, [§]Department of Materials Science and Engineering, and [⊥]Department of Macromolecular Engineering, Case Western Reserve University Schools of Medicine and Engineering, 10900 Euclid Avenue, Cleveland, Ohio 44106, United States

S *Supporting Information*

ABSTRACT: Nanomanufacturing of nanoparticles is critical for potential translation and commercialization. Continuous flow devices can alleviate this need through unceasing production of nanoparticles. Here we demonstrate the scaled-up production of spherical nanoparticles functionalized with biomedical cargos from the rod-shaped plant virus tobacco mosaic virus (TMV) using a mesofluidic, continued flow method. Production yields were increased 30-fold comparing the mesofluidic device versus batch methods. Finally, we produced MRI contrast agents of select sizes, with per particle relaxivity reaching 979,218 mM^{-1} s^{-1} at 60 MHz. These TMV-based spherical nanoparticle MRI contrast agents are in the top echelon of relaxivity per nanoparticle.

KEYWORDS: *nanomanufacturing, mesofluidic device, tobacco mosaic virus, nanoparticle shape, MRI contrast agents*
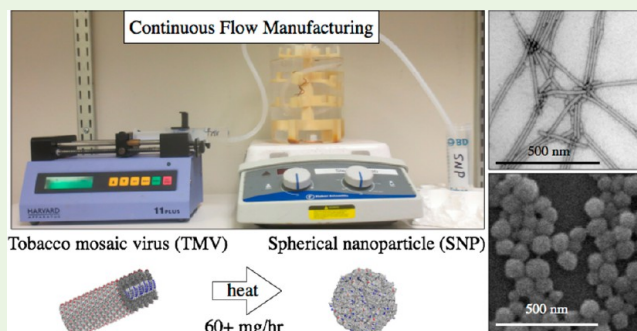
Viruses are highly symmetrical, nanoscale assemblies that consist of hundreds or thousands of identical coat proteins encapsulating their genomic material. Designed by nature, these genetically encoded biomaterials form with atomic precision and are highly monodisperse in shape and size. Because of their structural beauty, researchers have sought these nanoparticles for a variety of applications in nanotechnology/medicine. Plant virus-based platforms are of particular interest for nanomedicine because the proteinaceous scaffolds are noninfectious toward mammals, and they are biocompatible and biodegradable. The capsids serve as multivalent scaffolds amenable to genetic and chemical modification to impart new functionalities.[1−3]

(Plant) viruses come in a variety of shapes and sizes; their structures are dynamic, as their coat proteins can be self-assembled into varying geometries. For example, the 30 nm sized brome mosaic virus can be disassembled into coat proteins and reassembled around artificial cargos yielding hybrid core−shell nanoparticles with controlled sizes.[4] Not only can different-sized particles be generated but also geometries can be switched. The icosahedron cowpea chlorotic mottle virus (CCMV) coat proteins can self-assemble into tubular structures in the presence of artificial DNA molecules.[5] An interesting platform is also the tobacco mosaic virus (TMV), which has been a model viral nanoparticle platform for applications in energy, cell growth, vaccine development, disease imaging, and more.[6−8] Reconstitution experiments of TMV date back almost 60 years, yielding either disk-shaped or rod-shaped structures.[9] In plants, TMV forms a stiff and hollow

rod measuring 300 × 18 nm made up of 2,130 identical coat proteins encapsulating a single-strand RNA. It was shown that TMV rods can also be thermally reshaped into spherical nanoparticles (SNPs).[10]

Our interest in TMV and its SNPs lies in the opportunity to perform structure−function studies elucidating how nanoparticles of different sizes and shapes behave in vivo.[11,12] Understanding the fates of nanomaterials in vivo is an important milestone in their development for medical applications. Currently, virus-based materials are in preclinical testing as contrast agents for imaging cancer[13] and cardiovascular disease.[14] For example, we have developed TMV-based magnetic resonance imaging (MRI) contrast enhancement agents and demonstrated molecular MRI in a mouse model of atherosclerosis.[14] The proteinaceous TMV or SNP platform can be chemically modified to carry large payloads of paramagnetic contrast agents for MRI; and we synthesized SNPs with extraordinary high per particle T_1 relaxivities of 400 000 mM^{-1} s^{-1} at 60 MHz. The per particle T_1 is 5 orders of magnitude higher compared to clinical agents such as Gadovist.[12]

A roadblock to translation of (virus-based) nanomaterials into commercial products is the lack of control over synthesis and modification conditions at larger volumes and scales. Continuous flow technologies offer a unique and viable option
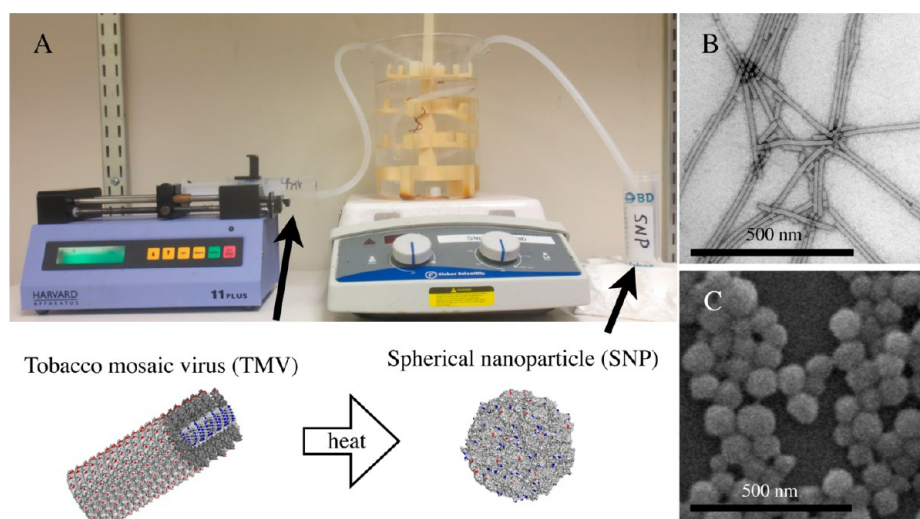
Figure 1. (A) Photograph of the mesofluidic device used to transition tobacco mosaic virus (TMV) rods to spherical nanoparticles (SNPs). (B) Transmission electron microscope image of TMV rods. (C) Scanning electron microscope image of SNPs.
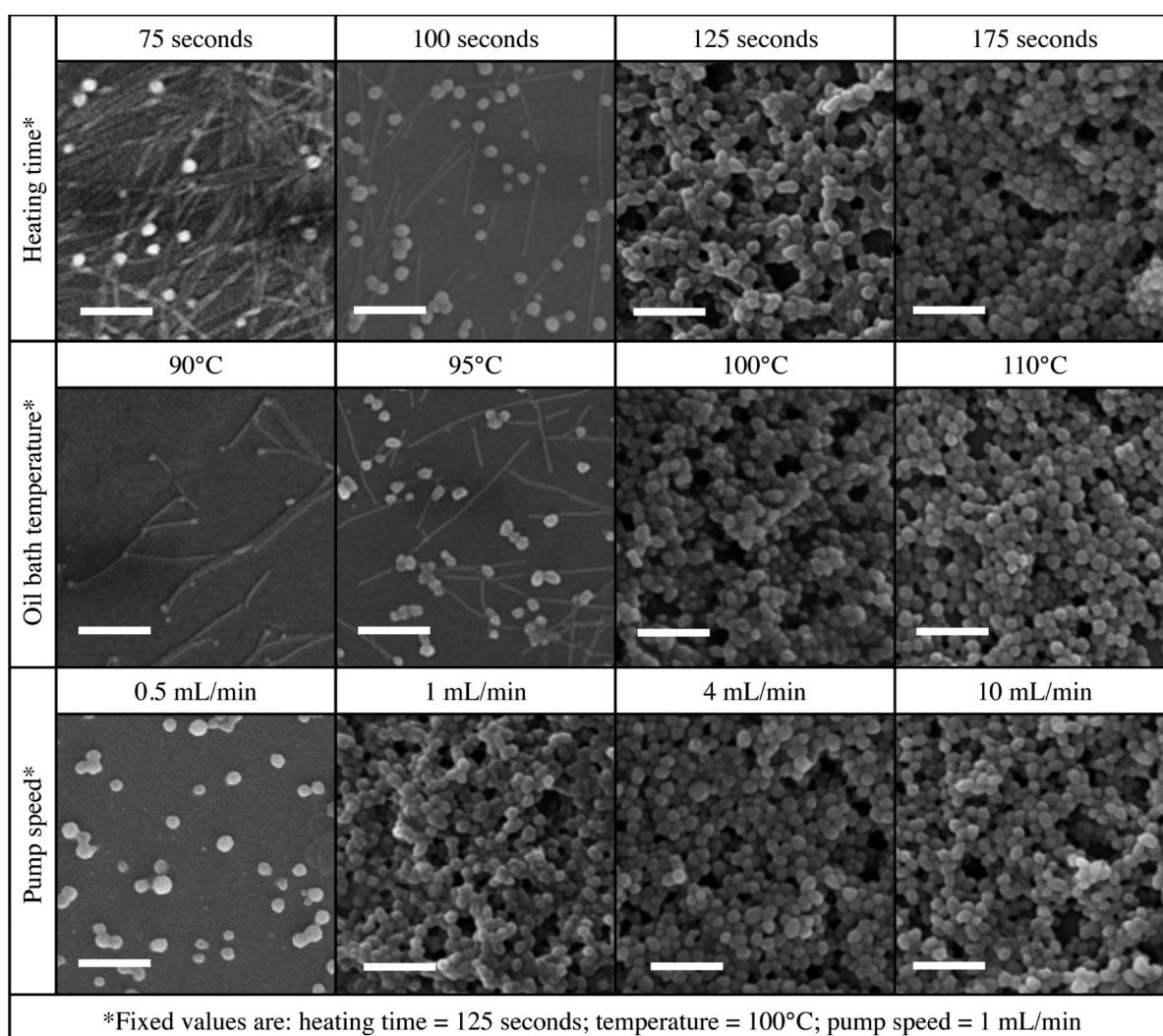

*Fixed values are: heating time = 125 seconds; temperature = 100°C; pump speed = 1 mL/min

Figure 2. SEM micrographs documenting SNP formulation using the mesofluidic device under various heating times (75−175 s), oil bath temperatures (90−110 °C), and pump speeds (0.5−10 mL/min). The scale bar is 500 nm.

to overcome this roadblock.[15,16] In this study, we set out to study the thermal shape transition of TMV into SNPs with the goal of automating the nanomanufacturing process using a mesoscale continuous flow device. SNPs are readily obtained

through heating TMV for 10 s at 94 °C;[10] SNP diameter is dictated by the concentration of TMV rods prior to heating, ranging from 50 to 800 nm. Although the manufacturing of TMV rods is scalable and economic through farming in plants, the thermal transition via batch method using a thermocycler is laborious, time-consuming, and wasteful. With a thermocycler, we obtained the best batch-to-batch reproducibility and complete thermal transition yielding uniform SNPs using 50 μL reaction volume of TMV at a concentration of 0.1 mg/mL with 96 tubes per run. Attempts to scale up production of SNPs by increasing reaction volume led to incomplete transition to SNPs from rods due to poor heat transfer (Figure S1). Increasing concentration led to increased SNP size. To overcome these challenges, we developed and tested a continuous flow mesofluidic device to produce SNPs (Figure 1A).

Continuous flow technologies offer a viable option for the scaled-up synthesis of nanoparticles.[15,16] Microfluidic devices (channel width <500 μm) offer a high degree of control over reaction conditions, but drawbacks include inherently small volumes, which limit flow rates and induce potential for clogging,[17,18] therefore reducing potential for scalability.[19] Mesofluidic devices (channel width >500 μm) are more scalable and have been utilized widely for the synthesis of small molecules;[18] and more recently mesofluidic devices have synthesized various inorganic nanoparticles.[20−24] Mesofluidic devices have several advantages over microfluidics; their simplicity, robustness of design, and scalability.[25] Optimized reaction parameters developed in a mesofluidic device can be translated directly to large-scale production without further optimization, which is in stark contrast to scaling up batch processing of microfluidic devices.[18]

Here, we established a protocol to transition TMV rods to SNPs under continuous flow using a custom mesofluidic device. Our mesofluidic device was designed for simplicity and versatility using common laboratory materials: a syringe pump drives a solution containing TMV rods through silicone tubing immersed in a hot oil bath; the solution is collected in centrifuge tubes for purification (Figure 1A). With an inner diameter of 1/8″, laminar flow dominates at all pump speeds tested here based on a Reynold's number of less than 2100 (Table S1). A tube holder was designed and produced using a 3D printer; the tube holder allowed placement of the tubing near the center of the oil bath to improve uniform heating (Figure 1A). Transmission and scanning electron microscopy (TEM and SEM, respectively) were used to confirm the size and morphology of TMV and SNPs before and after transition (Figure 1B, C). Further, UV−vis absorbance confirmed thermal transition from rods to SNPs; intact TMV has an A260:A280 ratio of 1.2; we found that upon transition to SNPs absorbance at 260 nm increases 2−3 times and the A260:A280 absorbance ratio increases to around 1.3 (Figure S2A and B). Therefore, change in UV−vis absorbance spectra provides a means to monitor SNP formation.[26]

A range of heating times, oil bath temperatures, and flow rates was tested to optimize the transition of TMV rods to SNPs under flow conditions (Figure 2). First, the parameter heating time was tested while pump speed (1 mL/min) and oil bath temperature (100 °C) were kept constant. Thermal transition to SNPs was confirmed by SEM imaging (Figure 2, top row); heating between 75s and 240s were considered. Data indicate 125s is minimal heating time (residence time in oil bath) required for complete transition of TMV rods into SNPs;

shorter heating times result in a mix of TMV rods and SNPs. Longer heating times of 150s (not shown) and 175s (Figure 2) had no effect on SNP size and morphology, indicating that once the thermal transition threshold is achieved, the SNPs are stable at 100 °C. Although a precise upper limit for heating time was not determined, we found that heating for 240s yielded no SNPs.

Further investigation into the thermal transition process using the PCR heat cycler revealed that formed SNPs are incredibly stable at 96 °C for extended periods of time (UV−vis absorbance shown in Figure S2 and SEM images in Figure S3). Initial reports indicated that 10s of heating at 96 °C using a PCR heat cycler produced SNPs from TMV rods;[10] with SNPs remaining intact following subsequent heating to 98 °C or freezing-thawing procedures. In our studies, we found that SNPs are stable for at least 25 min at 96 °C (Figures S2 and S3). It was previously demonstrated that surface modification of TMV rods with PEG$_{2K}$ molecules leads to increased thermal stability in buffered solutions as well as in organic solvents with thermal stability reported at 160 °C for 20 min.[27] It appears that transition of TMV rods into spheres also enhances its thermal stability, thereby providing a robust platform for chemical processing. Besides thermal stability, we also tested the stability of SNPs at room temperature in buffers with varying pH values and salt composition and concentration (Figure S4). We found that SNPs maintained their size and morphology for 3 weeks in all buffers tested, implying they are suitable for biomedical use.

Next, we optimized the oil bath temperature keeping pump speed at 1 mL/min and heating time at 125 s. Previous studies suggest that the reaction must reach 94−96 °C for 10s for thermal transition to occur in the PCR heat cycler.[10] Using our device, the minimum temperature threshold to yield uniform SNPs was found to lie at 100 °C; higher temperatures (110 °C) also yielded SNPs while lower temperatures (90 and 95 °C) resulted in TMV and SNP mixtures (Figure 2 middle row). Higher temperatures (110 °C) also yielded stable SNPs, further attesting to the thermal stability of the SNPs.

Finally, the parameter pump speed on TMV−SNP transition was evaluated. Heating time was kept at 125s and the temperature was set to 100 °C, while flow rates were varied between 0.50 mL/min and 10 mL/min. Consistent batch-to-batch transition from TMV to SNPs was confirmed for all flow speeds (Figure 2, bottom row). This is explained by the fact that flow is laminar under each condition tested (Table S1).

Using optimized conditions set at a speed of 10 mL/min, 100 °C, a heating time of 125s, and a 0.1 mg/mL solution of TMV, we achieved production up to 60 mg/h SNPs with good monodispersity and batch-to-batch consistency. These yields are comparable to reports by groups scaling up continuous flow synthesis of of inorganic nanoparticles.[24]

We evaluated the ability of the mesofluidic device to transition chemically modified TMV rods into functionalized SNPs. We tested various chemical modifiers including: biotin (a universal handle for purification or further functionalization via (strept)avidin), Cy5 and Gd(DOTA) as optical and MR imaging agents, and PEG M.W. 2000 Da (PEG$_{2K}$, a biocompatible polymer used to enhance pharmacokinetics of nanoparticles). We modified both the interior and exterior of the hollow TMV tube with these modifiers to demonstrate transition versatility (reaction schemes shown in Figure S5).

Specifically, we transitioned the following modified TMV rods to SNPs (Figure 3); interior modified Cy5 TMV (int-Cy5-
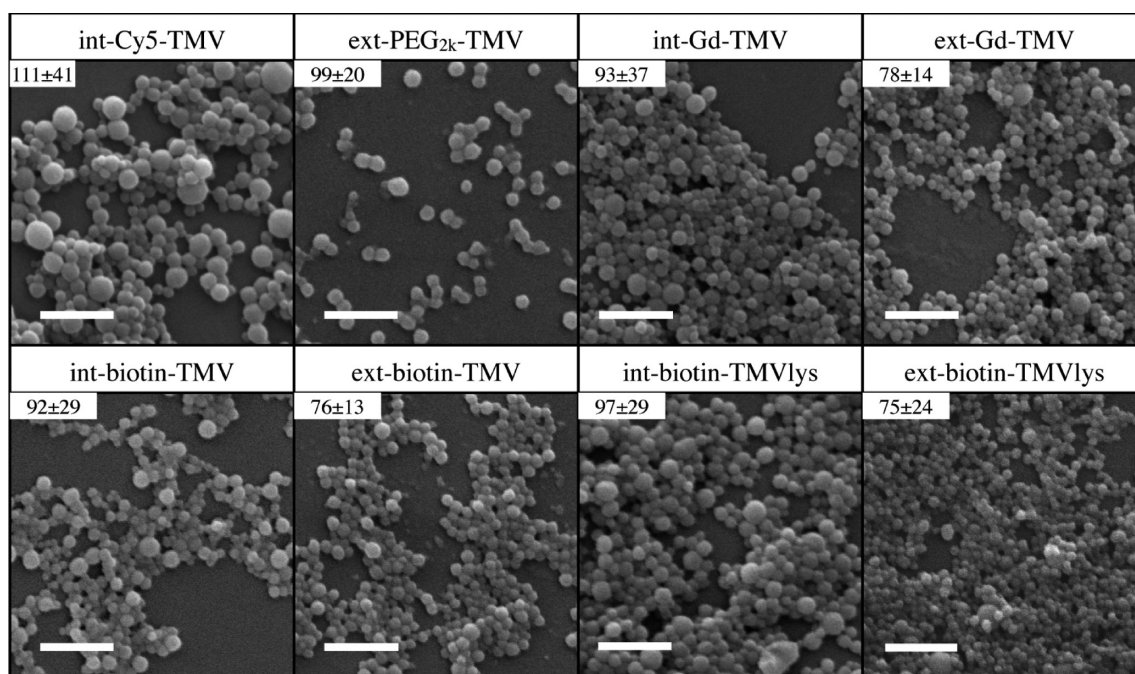
15

dx.doi.org/10.1021/ab500059s | ACS Biomater. Sci. Eng. 2015, 1, 13−18

Figure 3. SEM images of SNPs formed from chemically modified TMV particles. Inset shows average diameter and standard deviation. Scale bars are 500 nm.

TMV), exterior PEG modified TMV (ext-PEG$_{2k}$-TMV), interior or exterior Gd(DOTA) TMV (int-Gd-TMV, ext-Gd-TMV), interior or exterior biotin modified TMV (int-biotin-TMV, ext-biotin-TMV), a lysine mutant of TMV (TMVlys, specifically T158K) and interior or exterior biotin modified derivatives of TMVlys (int-biotin-TMVlys, ext-biotin-TMVlys). Functionalized TMV particles were characterized by mass spectrometry (Figure S6 and Table S2), SDS-PAGE, Western blotting against antibiotin (Figure S7), ICP-OES (for Gd), and TEM (Figure S8). Similar to native TMV, the absorbance at 260 nm of modified TMV particles increases following transition to SNPs (Figure S9). However, the degree of increase varies based on modification with no obvious trend observed. Additionally, modified TMV-to-SNP particles exhibited similar thermal stability upon extended heating time (Figure S9) and long-term stability able to remain at room temperature for at least 3 weeks (Figure S10).

Serendipitously, exterior tyrosine modified TMV (ext-PEG$_{2k}$-TMV, ext-Gd-TMV, ext-biotin-TMV) transitioned to SNPs successfully; somewhat contradicting our previous study using a thermocycler that suggested that modification of TYR139 on the TMV coat protein blocked SNP formation.[12] The longer heat exposure using the continuous flow method may enable the transition from rods to SNPs. It was noted that interior-modified TMV rods formed generally larger SNPs with larger size variation compared to exterior-modified particles, which formed smaller particles with lower size dispersity (Figure 3 inset shows size and dispersity). The exterior modified particles formed SNPs with similar size and polydispersity to native TMV. We attribute this to the tendency for interior modified TMV (modifying amino acids GLU97 and GLU106) to form longer rods (greater than 300 nm) with greater polydispersity in length due to stabilization of protein−protein interactions by neutralizing interior carboxylic acids after chemical modification.[28] Longer TMV rods will yield larger SNPs. Modifying exterior tyrosine (modifying amino acid TYR139) blocks the

head-to-tail assembly of TMV, which assures that the TMV rods are close to their original length of 300 nm.[29] We highlight that all formulations of TMV that passed through the mesofluidic device formed SNPs.

Finally, we show that the mesofluidic device is suitable to produce SNP-based MRI contrast agent of various sizes (and hence T_1 properties) by varying the starting TMV concentration. TMV with 952 Gd(DOTA) on its interior glutamic acid residues served as a starting material forming SNPs of select sizes using our mesofluidic device (Table 1). SNPs

Table 1. Physical and MRI Relaxivity Properties of Gd-SNPs; SNP size (nm), Gd per SNP as Determined by ICP-OES Measurement, And Longitudinal Ionic and Per Particle Relaxivity at 60 MHz (mM^{-1} s^{-1})

sample	size (nm)	Gd per NP	relaxivity per Gd (mM^{-1} s^{-1})	relaxivity per particle (mM^{-1} s^{-1})
Gd(DOTA)			5	5
iGd-TMV	300 × 18	952	23.9	22 721
0.1 mg/mL	58	837	21.6	18 067
1 mg/mL	88	3,905	22.3	87 094
2.5 mg/mL	188	33 059	25.4	838 079
5 mg/mL	218	46 569	21.0	979 218

formed from TMV at concentrations of 0.1, 1.0, 2.5, and 5.0 mg/mL resulted in SNPs with average diameters of 58 nm (837 Gd/SNP), 88 nm (3,905 Gd/SNP), 188 nm (33,059 Gd/SNP), and 218 nm (46,569 Gd/SNP), respectively (SEM shown in Figure S11). The ionic relaxivity remained relatively constant regardless of size; SNPs had ionic relaxivities ranging from 21.0 to 25.4 mM^{-1} s^{-1} at 60 MHz (Table 1). SNPs with diameters of 58, 88, 188, and 218 nm exhibited per particle relaxivities of 18,067, 87,094, 838,079, and 979,218 mM^{-1} s^{-1} at 60 MHz, respectively. This is the largest per particle relaxivity reported for a protein-based nanoparticle to date,[30] and in the

16

dx.doi.org/10.1021/ab500059s | ACS Biomater. Sci. Eng. 2015, 1, 13−18

same range as the highest relaxivity perfluorocarbon and silica nanoparticle MRI contrast agents.[30]

In conclusion, we demonstrate the nanomanufacturing of functionalized TMV-based SNPs, including MR contrast agents, using a continuous flow method with the following conditions: oil bath at or above 100 °C and heating times of at least 125s (at the mesoscale, pump speed is not a relevant parameter). Using this method, we can increase production of SNPs 30-fold from 2 mg/hour to 60 mg/hour while lowering costs and user input. Furthermore, we demonstrated that a variety of TMV rods functionalized with biomedical cargos can be transitioned to SNPs using the continuous flow method.

TMV provides a unique platform for bioengineering design; to date, it is the only macromolecular, virus-based platform reported to transition from a nanorod into a spherical nanoparticle upon heating. It would be interesting to test if this phenomenon could be replicated using other tubular biomaterials, such as other filamentous viruses, microtubules, amyloid fibrils, etc. Future studies could also set out to investigate whether mesofluidic synthesis of protein-based nanomaterials could be achieved from globular protein starting materials.

Virus-based, or more generally, protein-based materials, find applications in imaging, drug delivery, or vaccines. For translation of any novel (bio)material a key requirement, besides preclinical testing, is a scaled-up manufacturing protocol. The autonomous synthesis of nanoparticles with excellent batch-to-batch consistency is a need in their future commercialization and a critical step in improving the processability of nanoparticles. We envision mesofluidic nanoparticle manufacturing devices, based on the initial design here, capable of self-assembling, purifying, concentrating, and characterizing virus-based nanoparticle formulations with a single injection of precursors.

ASSOCIATED CONTENT

Ⓢ Supporting Information
The following file is available free of charge on the ACS Publications website at DOI: 10.1021/ab500059s.

Experimental protocols and supporting data (PDF)

AUTHOR INFORMATION

Corresponding Author
*E-mail: nicole.steinmetz@case.edu. Telephone: 216-844-8164.

Author Contributions
All authors contributed to the experimental design, data, and writing of the manuscript. All authors have given approval to the final version of the manuscript.

Notes
The authors declare no competing financial interest.

ABBREVIATIONS
TMV, tobacco mosaic virus; CCMV, cowpea chlorotic mottle virus; SNP, spherical nanoparticle; MRI, magnetic resonance imaging; TEM, transmission electron microscopy; SEM, scanning electron microscopy; UV−vis, ultraviolet−visible; ICP-OES, inductively coupled plasma optical emission spectroscopy; MALDI-TOF MS, matrix-assisted laser desorption-ionization time-of-flight mass spectrometry; PCR, polymerase chain reaction; DOTA, azido-mono amide-1,4,7,10-tetraazacyclododecane-N,N',N'',N'''-tetraacetic acid; PEG, polyethylene glycol

REFERENCES
(1) Li, F.; Wang, Q. Fabrication of nanoarchitectures templated by virus-based nanoparticles: strategies and applications. *Small* **2014**, *10* (2), 230−45.

(2) Wen, A. M.; Rambhia, P. H.; French, R. H.; Steinmetz, N. F. Design rules for nanomedical engineering: from physical virology to the applications of virus-based materials in medicine. *J. Biol. Phys.* **2013**, *39* (2), 301−25.

(3) Yildiz, I.; Shukla, S.; Steinmetz, N. F. Applications of viral nanoparticles in medicine. *Curr. Opin. Biotechnol.* **2011**, *22* (6), 901−908.

(4) Sun, J.; DuFort, C.; Daniel, M.-C.; Murali, A.; Chen, C.; Gopinath, K.; Stein, B.; De, M.; Rotello, V. M.; Holzenburg, A.; Kao, C. C.; Dragnea, B. Core-controlled polymorphism in virus-like particles. *Proc. Natl. Acad. Sci. U.S.A.* **2007**, *104* (4), 1354−1359.

(5) Mukherjee, S.; Pfeifer, C. M.; Johnson, J. M.; Liu, J.; Zlotnick, A. Redirecting the coat protein of a spherical virus to assemble into tubular nanostructures. *J. Am. Chem. Soc.* **2006**, *128* (8), 2538−9.

(6) Love, A. J.; Makarov, V.; Yaminsky, I.; Kalinina, N. O.; Taliansky, M. E. The use of tobacco mosaic virus and cowpea mosaic virus for the production of novel metal nanomaterials. *Virology* **2014**, *449*, 133−9.

(7) Alonso, J. M.; Gorzny, M. L.; Bittner, A. M. The physics of tobacco mosaic virus and virus-based devices in biotechnology. *Trends Biotechnol* **2013**, *31* (9), 530−8.

(8) Fan, X. Z.; Pomerantseva, E.; Gnerlich, M.; Brown, A.; Gerasopoulos, K.; McCarthy, M.; Culver, J.; Ghodssi, R. Tobacco mosaic virus: A biological building block for micro/nano/bio systems. *J. Vacuum Sci. Technol., A* **2013**, *31* (5), 050815.

(9) Fraenkel-Conrat, H.; Williams, R. C. Reconstitution of Active Tobacco Mosaic Virus from Its Inactive Protein and Nucleic Acid Components. *Proc. Natl. Acad. Sci. U.S.A.* **1955**, *41* (10), 690−8.

(10) Atabekov, J.; Nikitin, N.; Arkhipenko, M.; Chirkov, S.; Karpova, O. Thermal transition of native tobacco mosaic virus and RNA-free viral proteins into spherical nanoparticles. *J. Gen. Virol.* **2011**, *92* (2), 453−456.

(11) Bruckman, M. A.; Randolph, L. N.; VanMeter, A.; Hern, S.; Shoffstall, A. J.; Taurog, R. E.; Steinmetz, N. F. Biodistribution, pharmacokinetics, and blood compatibility of native and PEGylated tobacco mosaic virus nano-rods and -spheres in mice. *Virology* **2014**, *449*, 163−73.

(12) Bruckman, M. A.; Hern, S.; Jiang, K.; Flask, C. A.; Yu, X.; Steinmetz, N. F. Tobacco mosaic virus rods and spheres as supramolecular high-relaxivity MRI contrast agents. *J. Mater. Chem. B* **2013**, *1* (10), 1482−1490.

(13) Lewis, J. D.; Destito, G.; Zijlstra, A.; Gonzalez, M. J.; Quigley, J. P.; Manchester, M.; Stuhlmann, H. Viral nanoparticles as tools for intravital vascular imaging. *Nature Medicine* **2006**, *12* (3), 354−360.

(14) Bruckman, M. A.; Jiang, K.; Simpson, E. J.; Randolph, L. N.; Luyt, L. G.; Yu, X.; Steinmetz, N. F. Dual-modal magnetic resonance and fluorescence imaging of atherosclerotic plaques in vivo using vcam-1 targeted tobacco mosaic virus. *Nano Lett.* **2014**, *14* (3), 1551−8.

(15) Sebastian, V.; Arruebo, M.; Santamaria, J. Reaction Engineering Strategies for the Production of Inorganic Nanomaterials. *Small* **2014**, *10* (5), 835−853.

17

dx.doi.org/10.1021/ab500059s | *ACS Biomater. Sci. Eng.* 2015, 1, 13−18

(16) Valencia, P. M.; Farokhzad, O. C.; Karnik, R.; Langer, R. Microfluidic technologies for accelerating the clinical translation of nanoparticles. *Nat. Nanotechnol.* **2012**, *7* (10), 623−9.

(17) Capretto, L.; Carugo, D.; Mazzitelli, S.; Nastruzzi, C.; Zhang, X. Microfluidic and lab-on-a-chip preparation routes for organic nanoparticles and vesicular systems for nanomedicine applications. *Adv. Drug Delivery Rev.* **2013**, *65* (11−12), 1496−1532.

(18) Wegner, J.; Ceylan, S.; Kirschning, A. Ten key issues in modern flow chemistry. *Chem. Commun.* **2011**, *47* (16), 4583−4592.

(19) Jin, H. D.; Chang, C.-H. Continuous synthesis of SnTe nanorods. *J. Mater. Chem.* **2011**, *21* (33), 12218.

(20) Lin, X. Z.; Terepka, A. D.; Yang, H. Synthesis of Silver Nanoparticles in a Continuous Flow Tubular Microreactor. *Nano Lett.* **2004**, *4* (11), 2227−2232.

(21) Biswas, S.; Miller, J. T.; Li, Y.; Nandakumar, K.; Kumar, C. S. Developing a millifluidic platform for the synthesis of ultrasmall nanoclusters: ultrasmall copper nanoclusters as a case study. *Small* **2012**, *8* (5), 687−98.

(22) Li, Y.; Sanampudi, A.; Raji Reddy, V.; Biswas, S.; Nandakumar, K.; Yemane, D.; Goettert, J.; Kumar, C. S. Size evolution of gold nanoparticles in a millifluidic reactor. *ChemPhysChem* **2012**, *13* (1), 177−82.

(23) Shavel, A.; Cadavid, D.; Ibáñez, M.; Carrete, A.; Cabot, A. Continuous Production of Cu 2ZnSnS 4Nanocrystals in a Flow Reactor. *J. Am. Chem. Soc.* **2012**, *134* (3), 1438−1441.

(24) Mirhosseini Moghaddam, M.; Baghbanzadeh, M.; Sadeghpour, A.; Glatter, O.; Kappe, C. O. Continuous-Flow Synthesis of CdSe Quantum Dots: A Size-Tunable and Scalable Approach. *Chem.—Eur. J.* **2013**, *19* (35), 11629−11636.

(25) Bally, F.; Garg, D. K.; Serra, C. A.; Hoarau, Y.; Anton, N.; Brochon, C.; Parida, D.; Vandamme, T.; Hadziioannou, G. Improved size-tunable preparation of polymeric nanoparticles by microfluidic nanoprecipitation. *Polymer* **2012**, *53* (22), 5045−5051.

(26) Dobrov, E. N.; Nikitin, N. A.; Trifonova, E. A.; Parshina, E. Y.; Makarov, V. V.; Maksimov, G. V.; Karpova, O. V.; Atabekov, J. G. Beta-structure of the coat protein subunits in spherical particles generated by tobacco mosaic virus thermal denaturation. *J. Biomol Struct Dyn* **2014**, *32* (5), 701−8.

(27) Holder, P. G.; Finley, D. T.; Stephanopoulos, N.; Walton, R.; Clark, D. S.; Francis, M. B. Dramatic thermal stability of virus-polymer conjugates in hydrophobic solvents. *Langmuir* **2010**, *26* (22), 17383−8.

(28) Culver, J. N.; Dawson, W. O.; Plonk, K.; Stubbs, G. Site-directed mutagenesis confirms the involvement of carboxylate groups in the disassembly of tobacco mosaic virus. *Virology* **1995**, *206* (1), 724−30.

(29) Bruckman, M. A.; Niu, Z.; Li, S.; Lee, L. A.; Varazo, K.; Nelson, T. L.; Lavigne, J. J.; Wang, Q. Development of Nanobiocomposite Fibers by Controlled-Assembly of Rod-Like Tobacco Mosaic Virus. *Nanobiotechnology* **2007**, *3* (1), 31−39.

(30) Bruckman, M. A.; Yu, X.; Steinmetz, N. F. Engineering Gd-loaded nanoparticles to enhance MRI sensitivity via T(1) shortening. *Nanotechnology* **2013**, *24* (46), 462001.

18

dx.doi.org/10.1021/ab500059s | *ACS Biomater. Sci. Eng.* 2015, 1, 13−18